THE ROLE OF TEMPERATURE ON 1,3-DI-ISO-PROPYL-BENZENE CATALYTIC REACTIONS USING FCC CATALYSTS.

S. Al-Khattaf
Chemical Engineering Department, King Fahd University of Petroleum & Minerals, Dhahran, 31261, Saudi Arabia

Abstract

The present study reports the catalytic reactions of a gasoline range aromatic compound 1,3-di-iso-propyl-benzene (1,3-DIPB). Experiments are performed in a novel CREC Riser Simulator, a catalytic reactor that mimics the operating conditions of large-scale FCC units. Reaction testing involved different reaction times and temperatures, using USY-zeolites of different crystal sizes (0.4-μm and 0.9-μm). It is suggested that 1,3-DIPB dealkylates in two consecutive steps. 1,3-DIPB catalytic dealkylation is found to increase with reaction time, however, it does not appear to be affected by rising temperature. The main reaction products of 1,3-DIPB conversion (cumene, benzene, and propene) are shown to be a prime function of temperature. Time on stream (TOS) decay model is employed to model the experimental data. The present study suggests that due to the larger activation energy for cumene dealkylation compared to 1,3-DIPB dealkylation, the secondary cumene dealkylation reaction suppresses the primary 1,3-DIPB dealkylation reaction as temperature increases.

Key words: 1,3-di-iso-propyl-benzene, catalytic cracking, USY-zeolites, alkyl-benzenes, activation energy. cumene, benzene.

1. INTRODUCTION

Y-zeolites have been used extensively in fluid catalytic cracking (FCC) since the sixties. The commercial FCC catalysts are manufactured with USY zeolites dispersed in an amorphous silica-alumina matrix forming the 60-μm particles [1]. In these catalysts, most of the active sites are located within the zeolite pore structure. In order for the reaction to proceed, molecules have to diffuse through the large matrix pores into the zeolite crystals. As a result only certain hydrocarbon species with a molecular size smaller than a given dimension can penetrate the zeolite pore structure [2].

The aromatic content of gasoline is a major concern for refiners. Due to the new environmental regulation, both benzene content and total aromatic content of gasoline are limited to 1 vol % and 25 vol% respectively [3]. Since the FCC units are the largest contributor to the gasoline pool, aromatic formation and reactions during catalytic cracking have been a subject of extensive research [4,5].

The chemistry and kinetics of cumene catalytic cracking have received the largest attention from researchers due to its simplicity. Corma and Wojciechowski have reviewed this reaction in detail [6]. Long chain aromatics also draw the attention of researchers because they represent the aromatics in gas oil. Corma and Co-workers [4,5] reported that these compounds crack by a number of competing reaction pathways including dealkylation, side chain cracking and self alkylation. Watson et al [7], investigated the cracking of 1-phenylhexane, 1-phenyloctane and 1-phenyldecane. They concluded that the dominant pathways for cracking these aromatics included dealkylation and cracking of the side chain. However, dealkylation reaction became less dominant as alkyl side chain length increased.

Regarding the catalytic cracking of isopropyl-benzene, the main reaction pathway appears to be the cleavage of the propyl group from the benzene ring with the benzene ring remaining unaltered [6]. In addition and together with the cracking reaction there are some disproportionation, transalkylation, isomerization and coke formation (condensation reactions) [6,3]. However, most attention on cracking of these important aromatic compounds has focused on cumene due to it's simplicity and on 1,3,5,tri-iso-propyl-benzene (TIPB) to study the diffusion effect due to it's large size [8,9].

Al-Khattaf and de Lasa [10,11] studied 1,3,5-TIPB catalytic cracking in a riser simulator. It was suggested that 1,3,5-TIPB dealkylates in a series of three steps. The first one is 1,3,5-TIPB dealkylation to di-iso-propyl-benzene

(DIPB). The produced DIPB, then dealkylates to cumene which finally dealkyaltes to benzene. It was also found that each step is greatly influenced by reaction temperature and diffusion obstacles [10,11].

Regarding the diffusion of hydrocarbon molecules in zeolites, molecules should not be viewed as rigid bodies [12]. Even if the molecules critical diameters are greater than the USY-zeolite super cage, these hydrocarbon molecules can still manage to diffuse inside the zeolites. In this respect, molecules able to enter the zeolite structure can have a critical diameter as large as 10.2 Å [2,12]. For iso-propyl-benzene family, these molecules can diffuse and eventually crack inside the Y-zeolite structure. For example, it was found that cumene and 1,3-DIPB (with 6.4 Å and 8.4 Å critical diameters respectively) reactions using FCC catalysts containing USY-zeolite are not controlled by diffusion at reaction temperatures greater or equal to 400^{o}C [13,14].

Thus although cumene cracking has been used extensively as a test reaction to investigate the characteristics of newly developed cracking catalysts [6], limited research has been developed on the cracking of di-iso-propyl-benzene (DIPB). Cumene and DIPB are typical aromatic compounds in the gasoline pool. Thus the reactions of these important aromatics are quite significant for refiners. The important role of temperature on the formation and reactions of these aromatics (iso-propylbenzenes) needs to be investigated. In the present work, the catalytic cracking of 1,3-DIPB is studied under typical FCC conditions. The effect of temperature on 1,3-DIPB reactions is highlighted.

2. EXPERIMENTAL PROCEDURES

1,3-DIPB was employed as model reactant compound. Regarding the FCC catalysts, commercially available Y-zeolites (small and large crystals) from Tosoh Company were used. Properties of these zeolites are reported in Table 1. These Na-zeolites were ion exchanged with NH_4NO_3 to replace the sodium cation with the NH_4^+ cation. Following this, NH_3 was removed and the H form of the zeolites was spray-dried using kaolin as the filler and silica sol as the binder. The resulting 60-μm catalyst particles, with an essentially inactive matrix, had the following composition: 30 wt% zeolite, 50 wt% kaoline, and 20 wt% silica sol. The process of sodium removal was repeated for the pelletized catalyst. Following this, the catalyst was calcined for 2 hr at 600°C. Finally, the fluidizable catalyst particles (60-μm average size) were treated with 100% steam at 760°C for 5 hr. Table 2 reports the catalyst main properties following catalyst pretreatment. The unit cell size was determined by X-ray diffraction following ASTM D-3942-80. Surface area was measured using the BET method. It can be observed that, for both zeolites, the initial zeolite unit cell size of 24.5 Å was reduced, following steaming, to 24.28Å.

3. REACTION EVALUATION

The catalytic activity of the USY-zeolite catalyst, typically 0.81grams of catalyst, prepared using the various techniques described above, was measured in a novel CREC Riser Simulator using 1,3 di-iso-propyl-benzene (1,3-DIPB). The Riser Simulator is a new bench scale unit, invented by de Lasa [15]. This unit overcomes the technical problems of the standard micro-activity test (MAT) and has become a most valuable experimental tool for testing and developing new FCC catalysts [16-20].

The Riser Simulator consists of two outer shells: a lower shell and an upper shell. This design permits to load and to unload the catalyst easily. This reactor is designed in such way that an annular space is left between the outer portion of the basket and the inner walls of the reactor. A metallic gasket seals the two chambers. An impeller is located in the upper section of the unit. A packing gland assembly and a cooling jacket surround the shaft supporting the impeller. Upon rotation of the shaft, gas is forced outward from the center of the impeller towards the walls. This creates a lower pressure in the center region of the impeller thus inducing an up flow of gas through the catalyst chamber and a down flow in the reactor annular section. The motion of the fluid provides a fluidized bed of catalyst particles as well as intense gas mixing inside the reactor.

The Riser Simulator operates in conjunction with a series of sampling valves. This allows following a predetermined sequence, to inject hydrocarbons and to withdraw, using vacuum (typically 7 KPa) and at a pre-set time, all formed products. These time periods, between hydrocarbon injection and total product withdrawal, define the so-called contact time in the Riser Simulator. Thus, several independent experiments were developed to analyze the effect of contact time on conversion at a given reaction temperature. Mass balances for each one of these independent experiments closed in the 4+/-% range.

A Hewlett Packard 5890A GC helps on the quantification of fraction of reaction products. The GC is equipped with an FID detector and a capillary column HP-1, 25 m cross-linked methyl silicone with an outer diameter of 0.22 mm and an internal diameter of 0.33 microns. A more detailed description of various Riser Simulator components and the sequence of injection and sampling methods can be found in Pruski [21].

Regarding the specific conditions selected for the development of this study they were varied as follows: temperature: 450-550ºC, type of zeolite crystals= 0.4 microns (CAT-SC) and 0.9 micron (CAT-LC. The C/O ratio was set at 5 and total pressure was kept in the 170-240 KPa range. The C/O ratio as well as the total pressure were kept essentially constant during the experiments, at 5 and 206 KPa (+/-14%) respectively. Conversion, selectivities (amount of product formed /amount of reactant converted) and yields (amount of product formed/amount of reactant) reported are the average of at least 3 measurements. Typical errors in the conversion were in the +/-2% range.

4. RESULTS AND DISCUSSION

4.1 Cumene Reactions

To understand isopropyl-benzene reactions in FCC conditions, it is essential to study carefully cumene reactions under such circumstances. Grasping cumene reaction pathways can provide a vital base to understand multiple-isopropyl-benzene reactions in similar reaction conditions.

Cumene catalytic cracking was studied by numerous researchers. It was shown that cumene conversion consistently increased with both reaction time and reaction temperature [10,13,14]. However, it was observed that reaction temperature had a mild effect on cumene conversion with reaction times having a more significant influence. For instance, at 5 seconds, cumene conversions were 23%, 32%, 38.5% and 41% at 400°C, 450°C, 500°C and 550°C respectively [10,14].

It is well established that cumene disappears due to different reactions as follows;

1-cumene de-alkylation giving benzene and propene

2-cumene isomerization giving mainly n-propylbenzene and ethyl-toluene

3-cumene disproportionation giving di-isopropylbenzene and benzene

4-cumene side chain cracking

Cumene isomerization into n-propyl-benzene was observed to be negligible. The yield of n-propylbenzene was found to be around 1 wt% at 400^{o}C (5 sec reaction time) and increased to 1.5 wt% at 500^{o}C and 5 sec reaction time. Regarding cumene disproportionation, the existence of di-iso-propylbenzene (DIPB) in the product is a very good indication for the existence of such reaction [13]. However, this reaction was observed to be maximum at low reaction temperature and it's rate decreases with temperature in agreement with Best and Wojciechowski, [22]. Consistent with this, the observed DIPB mass fraction reached a maximum level of 1.6 wt% at 400^{o}C and 10 seconds and a minimum at 550^{o}C and 3 seconds (0.08 wt%).

Cumene dealkylation in the Riser Simulator was modeled using time–on-stream (TOS) and reactant conversion (RC) models [14]. Based on TOS model, activation energies in the range of 5.5-6.6 Kcal/mol were found for both CAT-SC and CAT-LC respectively. Deactivation constants of 0.17 and 0.19 (sec^{-1}) were reported for both catalysts. Based on reactant conversion (RC) model, activation energies in the range of 12.8-14.8 Kcal/mol were found for both CAT-SC and CAT-LC respectively. Deactivation constants of 5.5 and 6.2 were reported for both catalysts [14].

In conclusion, many reactions take place during cumene catalytic conversion using FCC catalysts and conditions. However, cumene dealkylation into benzene and propene is the dominant one and was observed to increase with both reaction temperature and reaction time. Thus, based on the present results, the highest cumene conversion was obtained at 550^{o}C and 10 sec reaction time [10,13,14].

4.2 1,3-DIPB Reactions

Figures 1a and 1b report the changes of 1,3-DIPB conversion as a function of reaction time (3 to 10 sec) and temperature (400 and 550°C) for both CAT-LC and CAT-SC respectively. It can be observed that for both catalysts and at all reaction temperatures, 1,3-DIPB conversions steadily increased with reaction time. Cumene, propene, and

benzene were the main products of the 1,3-DIPB conversions. However, it is very clear that the temperature effect on 1,3-DIPB conversion is negligible for all reaction times. The effect of reaction time on 1,3-DIPB conversions is expected and easy to understand. However, the role of temperature on 1,3-DIPB conversions needs more study and clarification.

It is hypothesized that 1,3-DIPB cracks in a two steps in-series reaction. The first step gives cumene and propene [6,10]. Then, cumene cracks forming, in a second step, benzene and propene. Figure 2 illustrates the two consecutive steps involved in 1,3-DIPB catalytic dealkylation.

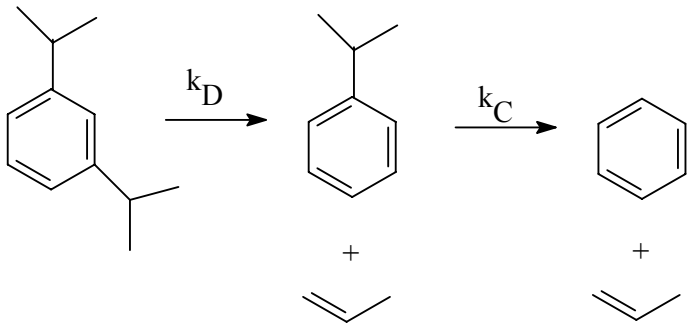

Figure 2. Schematic description of the catalytic dealkylation of 1,3-DIPB.

Where k_D and k_C are the rate constants of 1,3-DIPB dealkylation reaction and cumene dealkylation respectively. According to Arrhenius's Equation, $k_D = k_{D0}\ \exp(-E_D/RT)$ and $k_C = k_{C0}\ \exp(-E_C/RT)$ where E_D and E_C are the activation energies of 1,3-DIPB dealkylation and cumene dealkylation respectively. Of the total products formed, these three species (cumene, benzene and propene) amount to 85% and 84% at 400°C for 5 and 10 seconds reaction times respectively. At 550°C these species become 84% and 88% respectively. Consequently, as in the case of cumene [10,13,14], the de-alkylation reaction becomes more prevalent at the higher temperatures.

The other products in 1,3-DIPB catalytic dealkylation include toluene, ethylbenzene, n-propylbenzene, and cymene. Toluene was found to be negligible (less that 0.1 wt%). The formation of toluene, ethylbenzene, and cymene is a clear indication of the side cracking of the isopropyl group attached to the benzene ring. However, the three compounds combined to form less than 3 wt% of the total products. For example, the highest toluene yield (0.35 wt%) was detected at 10 sec reaction time and 550°C. Ethylbenzene highest yield was found to be around 1 wt% at 10 sec and 500°C. Finally cymene highest yield was found to be 0.6 wt % at 10 sec and 400°C.

The largest byproduct is methyl-DIPB, which contributes 3 to 5 wt% of the total products. The formation of ethylbenzene, cymene and methyl-DIPB is an indication of the transfer of methyl group from cumene and 1,3-DIPB to another 1,3-DIPB and cumene molecules to form methyl-DIPB and cymene. Thus each cymene and ethylbenzene molecule formed can lead to the formation of three methyl-DIPB molecules. This reaction is called disproportionation reaction [6]. However, methyl-DIPB is unstable and starts to disappear as soon as it forms (see Figure 3).

Para-DIPB forms through direct isomerization of 1,3-DIPB and has a weight fraction yield in the range of 0.2 wt% (at 550°C and 10 sec) and 2.3 wt% (at 400°C and 10 sec). It is clear that *Para*-DIPB starts to react as soon as it forms. Figure 4 shows that Para-DIPB yield decreases tremendously as the reaction temperature reaches 450°C until it reaches less than 0.3 wt% at 500 and 550°C. It can be noticed that at present reaction conditions 1,3-DIPB isomerization reactions can be neglected compared to the main 1,3-DIPB dealkylation reactions (Figure 2).

Thus based on the above discussion the other reactions involved in the 1,3-DIPB catalytic conversion such as disproportionation and isomerization are neglected in the present study. The main reaction in 1,3-DIPB disappearance is assumed to be the two-step dealkylation reactions as shown in Figure 2. This dealkylation pathway was tested in the present work. Cumene yield was observed to be an unstable intermediate product and benzene and propene were found to be the most important stable final products.

Figures 1a and 1b show that increasing reaction temperature from 400 to 500°C has increased 1,3-DIPB conversion from 51.3% to 52.3 % for CAT-LC and from 50.6% to 51.2% for CAT-SC (at 5 sec reaction time). This change in 1,3-DIPB conversion can be considered negligible and it is within the range of the experimental error. Therefore, increasing reaction temperature by 100°C has a negligible effect on 1,3-DIPB conversion. However, the product selectivities were noticed to respond differently to the change in reaction temperature. For example, at the same conditions of the above conversions, cumene yield was found to decrease from 23.4 wt% (for CATSC at 400°C and 5 sec) to 9.7 wt% at 500°C and 5 sec reaction time. CAT-LC also showed a similar trend for cumene yield by increasing temperature to 500°C, where cumene yield was decreased from 24 wt% to 12wt % at the same reaction time. The decline in cumene yield was always accompanied by an increase in both benzene and propene yields. Hence, in spite of the constant 1,3-DIPB conversion, cumene yield for both catalysts dropped by more than 50%. Figures 5a and 5b show cumene yield at different reaction times and temperatures for both catalysts.

These results show that for reaction temperature above 400°C 1,3-DIPB conversion is relatively insensitive to the reaction temperature. This suggests that as temperature increases, 1,3-DIPB molecules find difficulty to reach the catalyst surface. A similar phenomenon was reported by Satterfield [26] for hexene oxidation, where hexane conversion was found to be insensitive for temperature at 400-500°C. The reason for this behavior was attributed to the external mass transfer limitation.

Similarly for the present system, as temperature increases, 1,3-DIPB molecules are effectively consumed before it penetrate inside the zeolite pores. Consequently, the concentration difference between 1,3-DIPB in the bulk and on the catalyst surface becomes significant. This reaction regime is called external-diffusion regime and the rate limiting step in this regime is the mass transfer from the bulk to the catalyst surface [26]. Furthermore, the experimental results between the two crystal zeolites suggest that this reaction is not limited by pore diffusion. It was reported [10] that the conversion of 1,3-DIPB was not a function of Y-zeolite crystal size. The main criteria for this kind of diffusion is sensitivity to the zeolite crystal size [26].

Moreover, as temperature increases cumene, which already exists inside the zeolite pores, undergoes the secondary dealkylation reactions. It can be speculated that since a limited numbers of active sites are present inside the zeolite pores, most of these sites will be occupied by cumene inhibiting 1,3-DIPB from adsorption and reaction. Furthermore, products formation such as benzene, cumene, and other aromatics have to slow the advance of 1,3-DIPB molecules to the zeolite crystal (counterdifusion).

The above argument can be supported by the following reasoning; increasing temperature from 400 to 550°C leads to a decrease in cumene yield from 30 wt% to 5.2 wt% for CAT-SC and 10 sec reaction time (see Figures 5a and 5b). This decrease in cumene yield was simultaneously accompanied by an increase in benzene yield (see Figures 6a and 6b) from 3.6 wt% to 26 wt% and propene yield has increased from 14.5 wt% to 23 wt%. All these changes in cumene, benzene, and propene yields take place while 1,3-DIPB conversion has increased only from 60% to 62 % which can be considered as a negligible change. Furthermore, Figure 7 shows the increment in propene yield with reaction time and reaction temperature. These are clear signs for changing reaction paths with changing reaction temperature.

It can be concluded that the main reaction of 1,3-DIPB catalytic cracking using USY-zeolite catalysts includes two consecutive dealkylation steps. The first one is 1,3-DIPB dealkylation to cumene and propene. This step has been shown to increase with reaction time at all used temperatures. The increase in 1,3-DIPB conversion level was always accompanied by increase in cumene yield. For example, at 400°C, increasing reaction time from 3 to 10 sec increased the cumene yield from 18.5wt% to 30wt%, while, benzene yield increased from 3.7 wt% to 5.3 wt%.

The second step is the dealkylation of the produced cumene into benzene and propene. The present results suggested that this step increases with both reaction time (or 1,3-DIPB conversion) and reaction temperature. The main signs of increasing the rate of this step are;

1-Negligible change in overall 1,3-DIPB conversion.

2-Large decrease in cumene yield.

3-Large increase in both benzene and propene yields.

Finally, coke yield was found to be very low. Table 3 shows coke selectivity at different reaction conditions. It can be noticed that coke selectivity is within a range of 1 to 2 %. Hence coke selectivity can be neglected compared to benzene (10-50 %), cumene (60-10 %) and propene (20-35 %). However, it has to be stressed that neglecting coke as product, does not rule out the very important role of coking in catalyst deactivation. Little amount of coke is needed to completely or partially deactivate the catalyst. Hence coke deactivation was considered by introducing the deactivation function(φ) in the modeling part.

5. MODELING 1,3-DIPB CRACKING IN THE CREC RISER SIMULATOR

1,3-DIPB dealkylation is a first order reaction similar to cumene dealkylation. Its disappearance in the Riser Simulator can be represented by the following species balance equation;

$$-\frac{V}{W_c}\frac{dC_D}{dt} = k_D \varphi C_D \qquad (1)$$

where C_D represents 1,3-DIPB concentration in the Riser Simulator (kmole/m^3), V the volume of the riser (45.10^{-6} m^3), W_c the mass of catalyst ($0.81.10^{-3}$ kgcat), t the reaction time in seconds, φ the deactivation function, and k the intrinsic rate constant in m^3/kgcat.s.

Moreover, the concentration of 1,3-DIPB, C_D can be expressed by the following relationship;

$$C_D = \frac{y_D W_{hc}}{MW_D V} \qquad (2)$$

where y_D represents the 1,3-DIPB mass fraction, W_{hc} the total mass of hydrocarbons inside the riser ($0.16.10^{-3}$ kg), and MW_D is the 1,3-DIPB molecular weight (162 kg/kmole).

Furthermore, the reaction rate constant k_D can be expressed using an Arrhenius' relation as $k_D=k_{D0}\exp(-E_D/RT)$. Then, Equation (1) can be written as follows;

$$-\frac{V}{W_c}\frac{dy_D}{dt} = k_{D0}\exp(\frac{-E_D}{RT})\varphi y_D \qquad (3)$$

In addition, and in order to reduce parameter cross-correlation it is customary to adopt the following form of Equation (3):

$$-\frac{V}{W_c}\frac{dy_D}{dt} = k_{D0}\exp(\frac{-E_D}{R}[\frac{1}{T}-\frac{1}{T_0}])\varphi\ y_D \qquad (4)$$

where T_o represents the average temperature used in the reaction experiments.

a)-Cumene formation

Cumene dealkylation and formation from 1,3-DIPB are both first order reaction [6]. Cumene formation in the Riser Simulator can also be represented by the following species balance equation;

$$\frac{V}{W_c}\frac{dy_C}{dt} = \varphi\ (\nu_C k_{D0}\exp(\frac{-E_D}{R}[\frac{1}{T}-\frac{1}{T_0}])y_D - k_{C0}\exp(\frac{-E_C}{R}[\frac{1}{T}-\frac{1}{T_0}])y_C) \qquad (5)$$

ν_c is the stoichiometric coefficient for cumene formation from 1,3-DIPB dealkylation and it equals to the molecular weight of 1,3-DIPB (162 g/mole) divided by cumene molecular weight (120 g/mole). Cumene isomerization and disproportionation have been neglected from Equation (5). This omission is based on the very low cumene isomerization and disproportionation products (*meta*- DIPB , *para*-DIPB and n-propylbenzene) [13].

b)-Benzene formation

Benzene is mainly formed via cumene dealkylation (the second dealkylation step). Thus benzene formation can be represented by the following equation;

$$\frac{V}{W_c}\frac{dy_B}{dt} = \varphi\ \nu_B k_{C0} \exp(\frac{-E_C}{R}[\frac{1}{T}-\frac{1}{T_0}])y_C \quad (6)$$

ν_B is the stoichiometric coefficient for benzene formation from cumene dealkylation and it equals to the molecular weight of cumene (120 g/mole) divided by benzene molecular weight (78 g/mole).

c*)-Propene formation*

According to Figure 2 propene can be formed through two different reactions. The first one is from the dealkylation of 1,3-DIPB. The second one is from cumene dealkylation [6]. Its formation in the Riser Simulator can also be represented by the following species balance equation;

$$\frac{V}{W_c}\frac{dy_p}{dt} = \varphi\ (\nu_{pD} k_{D0} \exp(\frac{-E_D}{R}[\frac{1}{T}-\frac{1}{T_0}])y_D + \nu_{pC} k_{C0} \exp(\frac{-E_C}{R}[\frac{1}{T}-\frac{1}{T_0}])y_C) \quad (7)$$

ν_{PD} is the stoichiometric coefficient for propene formation from 1,3-DIPB dealkylation and it equals to the molecular weight of 1,3-DIPB (162 g/mole) divided by propene molecular weight (42 g/mole). ν_{PC} is the stoichiometric coefficient for propene formation from cumene dealkylation and it equals to the molecular weight of cumene (120 g/mole) divided by propene molecular weight (42 g/mole).

d*)- Time-on-stream (TOS) decay model*

One classical approach, while describing catalyst decay is to consider catalyst decay as a function of time-on-stream. Time on stream (TOS) which is an empirical model assumes that coking rate is independent of reactant composition, extent of conversion, and hydrocarbon space velocity [23].

$\varphi = \exp(-\alpha t)$ [24]. (8)

where α is a constant and t is the time the catalyst is exposed to a reactant atmosphere (time –on-stream).

By substituting Equation (8) into Equations (4-7), the following is obtained:

$$-\frac{V}{W_c}\frac{dy_D}{dt} = k_{D0} \exp(\frac{-E_D}{R}[\frac{1}{T}-\frac{1}{T_0}]) \exp(-\alpha t) y_D \quad (9)$$

$$\frac{V}{W_c}\frac{dy_C}{dt} = (\nu_C k_{D0} \exp(\frac{-E_D}{R}[\frac{1}{T}-\frac{1}{T_0}])y_D - k_{C0} \exp(\frac{-E_C}{R}[\frac{1}{T}-\frac{1}{T_0}])y_C) \exp(-\alpha t) \quad (10)$$

$$\frac{V}{W_c}\frac{dy_B}{dt} = (\nu_B k_{C0} \exp(\frac{-E_C}{R}[\frac{1}{T}-\frac{1}{T_0}])y_C) \exp(-\alpha t) \quad (11)$$

$$\frac{V}{W_c}\frac{dy_p}{dt} = (\nu_{pD} k_{D0} \exp(\frac{-E_D}{R}[\frac{1}{T}-\frac{1}{T_0}])y_D + \nu_{pC} k_{C0} \exp(\frac{-E_C}{R}[\frac{1}{T}-\frac{1}{T_0}])y_C) \exp(-\alpha t) \quad (12)$$

Thus, the catalyst activity decay model, based on time on stream, given by Equations (9-12) involves five parameters k_{D0}, k_{C0}, E_D, E_C and α.

These five model parameters were determined using non-linear regression (MATLAB package). Table 3 reports the parameters obtained and the limited spans for the 95% confidence interval for CAT-LC. Table 4 indicates the very low correlation between k_{DO} and E_D, E_D and α and the moderate correlation between k_{D0} and α. The adequacy of the model and of the selected parameters to fit to data is shown in Table 3 given the 0.94-0.97 regression coefficients.

6. MODEL RESULTS

Based on TOS decay model φ was approximated as $\exp(-\alpha t)$ where α was found to be in the range of 0.193-0.21 (1/sec) for both CAT-LC and CAT-SC. Thus α can be averaged at around 0.2 (1/sec) for 1,3-DIPB catalytic conversion for the present experimental conditions. Based on the above calculation, φ equals 0.55, 0.368, 0.25 at 3, 5, and 7 sec reaction times respectively. It is important to mention that these values are the same for 400-550°C temperature range.

Figures 8a to 8d indicate the trend of the two consecutive dealkylation steps as function of time for 400, 450, 500, and 550°C respectively. It can be observed from these figures that 1,3-DIPB mass fraction curve has the same values for all temperatures and only changes with reaction time. It is obvious that the model reasonably predicts the 1,3-DIPB mass fractions with small deviations due to the experimental errors and due to the other reactions involved in 1,3-DIPB catalytic dealkylation that have been neglected. Cumene formation, on the other hand, was shown to change with both reaction times and temperatures. At 400°C, cumene formation curve is much higher than both benzene and propene formation curves (Figure 8a). This is a clear indication that at 400°C, the first dealkylation reaction rate is higher than the second dealkylation reaction. However, as reaction temperature increases to 450°C (Figure 8b), cumene formation declines, increasing both benzene and propene formation. Thus the temperature increment has suppressed the first dealkylation reaction and favored the second dealkylation reaction. At 500°C and 5 sec reaction time both curves (cumene and benzene formations) overlaps each other indicating that at these conditions, the rate of both dealkylation reactions are approximately equal as shown in Figure 8c. As temperature continues to increase to 550°C, propene and benzene become the dominant product at the expense of cumene as shown in Figure 8d.

It is very interesting to compare the values of E_D and E_C. The activation energy of cumene dealkylation E_C (15 kcal/mole) is almost 15 times higher than that of 1,3-DIPB dealkylation E_D (0.88-1 Kcal/mole). It is very well known that high activation energies are more sensitive to temperature than low activation energies. Levenspiel [25] reported that at 400°C, for E = 15.5 kcal/mole the rate of reaction doubled by increasing the temperature by 65°C. However, for E = 38.5 kcal/mole it requires a temperature increment of only 16°C to double the reaction rate. Therefore the difference in the activation energies of different reaction steps plays a significant role in determining the whole reaction behavior.

Another interesting point to notice is the activation energy of cumene dealkylation E_C. For pure cumene, Al-Khattaf and de Lasa, [14] found the activation energy of cumene dealklation to be 5.5-6.5 Kcal/mole for both catalysts (CAT-LC and CAT-SC). However, in the present study, where cumene was an intermediate product, the activation energy for the same reaction has increased to 15 Kcal/mole. It has to be noticed that cumene dealkylation is the primary reaction in the first case [14] and secondary reaction in the second case (the present study).

Finally, it is very important to mention that the kinetic constants for cumene dealkylation are in the range of the published results. Table 6 shows some of these values. However, for 1,3-DIPB dealkylation, no kinetic studies have been reported.

7. CONCLUSIONS

a. The catalytic reactions of 1,3-DIPB are successfully investigated in a novel CREC Riser Simulator under different reaction times and various temperatures using USY-zeolites of different sizes: CAT-SC (0.4-μm) and CAT-LC (0.9-μm).

b. The dealkylation of 1,3-DIPB into cumene, benzene and propene was shown to be the predominant reaction pathway under FCC conditions.

c. Changing reaction temperature between 400 and 550°C displays no effect on 1,3-DIPB conversion for both catalysts. Conversion was found to increase only with reaction time.

d. Changing reaction temperature between 400 and 550°C has a great effect on the secondary reaction of cumene dealkylation. This influence was shown by changing both benzene and cumene yields with temperature for the two catalysts. This behavior of the two series dealkylation steps was attributed to the external mass transfer.

e. The activation energy of cumene cracking as second consecutive step (15 kcal/mol) was found to be much greater than cumene cracking as pure feed or as first step (5.5-6.5 kcal/mol).

f Kinetic model for the two consecutive step 1,3-DIPB reactions was developed. The model parameters were estimated using regression analysis, with parameters established with their respective confidence intervals. The consistency of the kinetic parameters for the two-zeolite crystals is an encouraging result to support the validity of the proposed model.

g The 1,3-DIPB conversion was found not to be affected much with changing USY-zeolite crystal size. This suggests that this reaction is not limited by pore diffusion.

ACKNOWLEDGMENTS

The author would like to express his appreciation to the King Fahd University of Petroleum & Minerals (KFUPM) for their support. The author would like to acknowledge the support of Dr A. Humphries from Akzo Nobel and of J. Macaoay from Engelhard companies, who contributed significantly to this study with the preparation of the catalysts.

NOTATION

k_D intrinsic kinetic constant for cracking of 1,3-DIPB (m^3/Kgcat.s).

k_{D0} pre-exponential factor for the intrinsic reaction constant (m^3/Kgcat.s)

k_C intrinsic kinetic constant for cracking of cumene (m^3/Kgcat.s).

k_{C0} pre-exponential factor for the intrinsic reaction constant (m^3/Kgcat.s)

E_D energy of activation for the cracking reaction of 1,3-DIPB (kJ/mole).

E_C energy of activation for the cracking reaction of cumene (kJ/mole).

R universal gas constant (kJ/mol.K).

T temperature (K).

ϕ deactivation function (-).

ρ_c zeolite density (kg/m^3).

REFERENCES

[1] R. Sadeghbeigi, "Fluid Catalytic Cracking Hand Book, Design, operation, and Troubleshooting of FCC Facilities", *Gulf, New York*, (1995).

[2] J. Karger and D.M Ruthven, "Diffusion in Zeolites and Other Microporous Solids", John *Wiley & Sons, Inc*, (1992).

[3] T. Tsai, S. Liu, and I. Wang, "Disproportionation and Transalkylation of Alkylbenzenes over Zeolite Catalysts", *Appl. Catal*., *A* **181** (1999) pp. 181– 355.

[4] A. Corma, P.J Miguel, A.V. Orchilles, G. Koermer, and R. Madon, "Cracking of Long-Chain Alkyl Aromatics on USY Zeolite Catalysts", *J. Catal*., **135** (1992), pp. 35 – 45.

[5] A. Corma, P.J Miguel, A.V. Orchilles and G. Koermer, "Zeolite effect on Cracking of Long-Chain Alkyl Aromatic", *J. Catal.*, **145** (1994), pp. 181–186.

[6] A. Corma, and B.W Wojciechowski, "The Catalytic Cracking of Cumene", *Catal. Rev.-Sci. Eng*., **24** (1982), pp. 1– 65.

[7] B.A. Watson, M.T. Klein, and R.H. Harding, "Catalytic Cracking of Akylbenzene: Modeling the Reaction Pathways and Mechanisms", *Appl. Catal. A*, **160** (1997), pp. 13 – 39.

[8] E.F. Aguiar, M.L. Murta Valle, M.P. Silva, and D.F. Silva, "Influence of External Surface Area of Rare-Earth Containing Y zeolites on the Cracking of 1,3,5- triisopropylbezene", *Zeolites*, **15** (1995), pp. 620 – 623.

[9] K. Roos, A. Liepold, H. Koch, and W. Reschetilowski, "Impact of Accessibilty and Acidity on Novel Molecular Sieves for Catalytic Cracking of Hydrocarbons", *Chem. Eng. Technol*. **20** (1997), pp. 326 – 332.

[10] S. AL-Khattaf, and H.I de Lasa, "The Role of Diffusion on Alkyl-benzenes Catalytic Cracking", *Appl. Catal., A*, **226** (2002), pp. 139 – 153.

[11] S. AL-Khattaf, J. Atias, K. Jarosch, and H.I de Lasa, "Diffusion and catalytic cracking of 1,3,5 tri-iso-propyl-benzene in FCC catalysts" *Chem. Eng. Sci.* **57** (2002), pp. 4909 – 4920.

[12] J. Xiao, and J. Wei, "Diffusion Mechanism of Hydrocarbons in Zeolites 1. Theory", *Chem. Eng.* Sci. **47** (**5**) (1992), pp. 1123 – 1141.

[13] S. Al-Khattaf, "Diffusion and Reactions of Hydrocarbon in FCC Catalysts" *Ph.D Dissertation,* University of Western Ontario, London, Ontario, Canada, (2001).

[14] S. AL-Khattaf, and H.I de Lasa , "Catalytic Cracking of Cumene in a Riser Simulator: A Catalyst Activity Decay Model", *Ind. Eng. Chem. Res*.**40** (**23**) (2001), pp. 3598 – 5404.

[15] H.I de Lasa, *USA Patent* **5**, **102, 628** (1991).

[16] S. AL-Khattaf and H.I de Lasa, "Activity and Selectivity of Fluidized Catalytic Cracking Catalysts in a Riser Simulator: The Role of Y-Zeolite Crystal Size" *Ind. Eng. Chem. Res*. **38** (**4**) (1999), pp. 1350 – 1356.

[17] J.M. Arandes, I. Abajo, I. Lopez-Valerio, D.I. Fernandez, M.J. Azkoiti, M. Olazar , and J. Bilbao, "Transformation of Several Plastic Wastes into Fuels by Catalytic Cracking' *Ind. Eng. Chem. Res.* **36** (**11)** (1997), pp. 4523 – 4529.

[18] C.M. Bidabehere, and U. Sedran, "Simultaneous Diffusion, Adsorption, and Reaction in Fluid Catalytic Cracking Catalysts" *Ind. Eng. Chem. Res.* **40** (**2**) (2001), pp. 530 – 535.

[19] U. Sedran, *Catal. Rev. Sci*. Eng. "Laboratory testing of FCC catalysts and hydrogen transfer properties evaluation" **36**(**3**) (1994), pp. 405 – 431.

[20] J.M. Arandes, I. Abajo, I. Fernandez, M.J. Azkoiti, and J. Bilbao, *Ind. Eng. Chem. Res* "Effect of HZSM-5 Zeolite Addition to a Fluid Catalytic Cracking Catalyst. Study in a Laboratory Reactor Operating under Industrial Conditions", **39** (**6**) (2000), pp. 1917 – 1924.

[21] J. Pruski, " Catalytic Cracking of Hydrocarbons in a Novel Riser Simlator: Adsorption Phenomena", *MESc Thesis*, Univ. Western Ontario, London, Ontario, Canada, (1995).

[22] D. Best, and W. Wojciechowski, "On Identifying the Primary and Secondary Products of the Catalytic Cracking of Cumene", *J.Catal*., **47** (1977), pp. 11 – 27.

[23] S.J. Yates, "Fundamentals of Fluidized Bed Chemical Processes" *Butlewood Monographs in Chemical Engineering,* London, England, (1983), pp. 121.

[24] V.W. Weekman, " A Model of Catalytic Cracking Conversion in Fixed, Moving and Fluid-bed Reactors", *Ind. Eng. Chem. Proc. Des. Dev*., **7** (1968), pp. 90 – 95.

[25] O. Levenspiel, "Chemical Reaction Engineering", *Second edition, John Wiley & Sons Inc.,* New York (1972).

[26] C. Satterfield, "Heterogeneous Catalysis in Industrial Practice*", Second edition, McGraw-Hill, Inc.,* New York (1991)

[27] D.R. Acharya, R. Hughes, and K. Li, " Deactivation of Silica-Alumina Catalyst During the Cumene Cracking Reaction", *Appl. Catal. A*, **52** (1989) pp. 115 – 159.

Figures Captions

Figure 1a. 1,3-DIPB dealkylation. Effect of contact time and reaction temperature on 1,3-DIPB conversion (CAT-LC). (O) 3 sec, (□) 5 sec, (Δ) 7 sec, (◇) 10 sec.

Figure 1b. 1,3-DIPB dealkylation. Effect of contact time and reaction temperature on 1,3-DIPB conversion (CAT-SC). (●) 3 sec, (■) 5 sec, (▲) 7 sec, (◆) 10 sec.

Figure 2**.** Schematic description of the catalytic dealkylation of 1,3-DIPB.

Figure 3. The effect of reaction time and temperature on methyl-DIPB yield (CAT-LC).

Figure 4. The effect of reaction time and temperature on Para-DIPB yield (CAT-LC).
(O) 3 sec, (□) 5 sec, (Δ) 7 sec, (◇) 10 sec.

Figure 5a. The effect of reaction time and temperature on cumene yield (CAT-LC).
(O) 3 sec, (□) 5 sec, (Δ) 7 sec, (◇) 10 sec.

Figure 5b. The effect of reaction time and temperature on cumene yield (CAT-SC).
(●) 3 sec, (■) 5 sec, (▲) 7 sec, (◆) 10 sec.

Figure 6a. The effect of reaction time and temperature on benzene yield (CAT-LC).
(O) 3 sec, (□) 5 sec, (Δ) 7 sec, (◇) 10 sec.

Figure 6b. The effect of reaction time and temperature on benzene yield (CAT-SC).
(●) 3 sec, (■) 5 sec, (▲) 7 sec, (◆) 10 sec.

Figure 7. The effect of reaction time and temperature on propene yield (CAT-LC).
(O) 3 sec, (□) 5 sec, (Δ) 7 sec, (◇) 10 sec.

Figure 8a. Reaction of 1,3-DIPB. Change of product yields with reaction time at 400°C and C/O =5 for CAT-LC (TOS model). (□)1,3-DIPB, (O) cumene, (Δ) propene, (◇) benzene.

Figure 8b. Reaction of 1,3-DIPB. Change of product yields with reaction time at 450°C and C/O =5 for CAT-LC (TOS model). (□)1,3-DIPB, (O) cumene, (Δ) propene, (◇) benzene.

Figure 8c. Reaction of 1,3-DIPB. Change of product yields with reaction time at 500°C and C/O =5 for CAT-LC (TOS model). (□)1,3-DIPB, (O) cumene, (Δ) propene, (◇) benzene.

Figure 8d. Reaction of 1,3-DIPB. Change of product yields with reaction time at 550°C and C/O =5 for CAT-LC (TOS model). (□)1,3-DIPB, (O) cumene, (Δ) propene, (◇) benzene.

Table 1.
Properties of the small and large zeolite crystals of this study

	Small zeolite	Large zeolite
Na_2O (wt%)	4.1	0.25
SiO_2/Al_2O_3 (mol/mol)	5.6	5.7
Unit cell size (Å)	24.49	24.51
Crystal size (μm)	0.4	0.9

Table 2.
Properties of CAT-SC and CAT-LC catalysts used in this study

	CAT-SC	CAT-LC
Unit cell size (Å)	24.28	24.28
BET Surface Area (m^2/g)	148	155
Na_2O (wt%)	Negligible (1)	Negligible (1)
Crystal Size (μm)	0.4	0.9

(1) smaller than the SEM-EDX detectable levels of 0.001%

Table 3.

Coke selectivities for different reaction conditions (CAT-LC)

Conditions	Coke yield wt%	Coke selectivity ((coke yield g/1,3DIPB convert g) X 100) %
5 sec and 450C	0.10	1.0
5 sec and 500C	0.11	1.0
5 sec and 550C	0.12	1.25
10 sec and 400C	0.08	0.81
10 sec and 450 C	0.12	1.04
10 sec and 500 C	0.17	1.43
10 sec and 550 C	0.16	1.35

Table 4

Kinetic constants based on time on stream for CAT-LC

$k_{Do}.10^3$ m^3/kgcat.s	95% CFL	E_D kcal/mole	95% CFL	$k_{Co}.10^3$ m^3/kgcat.s	95% CFL	E_C kcal/mole	95% CFL	α 1/sec	95% CFL	r^2
1.21	0.18	0.88	0.33	3.74	0.87	15.26	3.5	0.2	0.06	0.974

Table 5

Correlation matrix for CAT-LC

	k_{D0}	E_D	k_{C0}	E_C	α
k_{D0}	1	0.148	0.57	-0.094	0.944
E_D	0.148	1	-0.089	-0.007	0.004
K_{C0}	0.57	-0.089	1	0.37	0.65
E_C	-0.094	-0.007	0.37	1	0.05
α	0.944	0.004	0.65	0.05	1

Table 6.

Some published studies of cumene catalytic cracking reaction

Reactor type	Catalyst	Activation energy (Kcal/mol)	Ref
Microcatalytic	Decationized Zeolite	14.5	6
Microcatalytic	Decationized Zeolite	18.0	6
Microcatalytic	LaY-Zeolite	17.0-18.0	6
Microcatalytic	Amorphous SiAl	15.0	6
Integral	Silica Alumina	11.1	6
Integral	LaY	19.5	6
Integral	Y-zeolite	20.0	6
Microcatalytic	Silica Alumina	8.51	27
Present study	Y-zeolite + Silica Alumina	15.5	